

# GOODS, UDF, and the evolution of early-type galaxies

I. Ferreras<sup>1,2</sup>, T. Lisker<sup>1,3</sup>, A. Pasquali<sup>1</sup>, C. M. Carollo<sup>1</sup>, S. J. Lilly<sup>1</sup> and B. Mobasher<sup>4</sup>

1. *Institut für Astronomie, ETH-Zürich, CH-8093 Zürich, Switzerland*

2. *Dept. Physics & Astronomy, UCL, Gower Street, London WC1E 6BT, United Kingdom*

3. *Astronomisches Institut, Universität Basel, Venusstrasse 7, CH-4102 Binningen, Switzerland*

4. *STScI, 3700 San Martin Drive, Baltimore, MD 21218, USA*

**Abstract.** The HST/ACS images of GOODS-South have been used to select a sample of early-type galaxies, based on morphology and on the Kormendy relation. The classification scheme does not use galaxy colours, hence it does not bias against young stellar populations. The 249 galaxies ( $i_{AB} < 24$ ) paint a complex formation picture. Their stellar populations show gradients which readily rule out a large range of ages among and within galaxies. On the other hand, there is a decrease in the comoving number density, which suggests a strong bias when comparing local and distant early-type galaxies. This bias can be caused either by a significant fraction of non early-type progenitors or by a selection effect (e.g. dust-enshrouded progenitors). The deep images of the UDF were used to determine the structural properties of some of these galaxies. Regarding the distribution of disk/boxy isophotes, we do not find large differences with respect to local systems. However, some early-types with the standard features of a red and dead galaxy reveal interesting residuals, possible signatures of past merging events.

## 1 Introduction

The star formation history of a galaxy is strongly dependent on its morphology, a mechanism which is well-known since the early days of observational cosmology. An accurate classification of morphologies is therefore key to a complete picture of galaxy formation and evolution. Of all morphologies, early-type systems dominate the high-mass end and pose one of the most intriguing riddles to our understanding of structure formation. Their old stellar components and tight scaling relations are in remarkable contrast with the extended assembly histories expected for such objects within the current paradigm of galaxy formation (e.g. White & Rees 1978). The inherent hierarchical nature of structure formation implies the more massive systems assemble at later times. The presence of massive distant red galaxies at high redshift (Förster-Schreiber, et al. 2004) or the peculiar abundance ratios in the stellar populations of early-type galaxies (Thomas, 1999) can only be reconciled if the “baryon physics” of gas collapse, star formation and feedback is not accounted for in an accurate way, so that the assembly and the formation histories are decoupled. Indeed, the “downsizing” effect observed in the formation of spheroidal galaxies (e.g. Treu, et al. 2005) implies that the baryon physics introduces an “inverted hierarchy”. The determination of the star formation and assembly histories of early-type galaxies thereby constitute one of the cornerstones of observational cosmology.

This contribution presents work done on the selection of early-type galaxies in one of the deepest and widest surveys currently available: the HST/ACS images of the GOODS survey (Giavalisco et al. 2004). The depth and spatial resolution of the images enabled us to perform a careful morphological classification. The deeper 12 arcmin<sup>2</sup> Ultra Deep Field (Beckwith, et al. 2005, in preparation) overlaps with the GOODS/CDFS region, and the spheroidal galaxies in this field can be explored in more detail. We present here some highlights of the sample. We refer interested readers to Ferreras et al. (2005) for the details of the analysis of the GOODS/CDFS sample and to Pasquali et al. (2005) for details of the UDF sample. A concordance  $\Lambda$ CDM cosmology ( $\Omega_{\Lambda} = 0.7$ ,  $\Omega_m = 0.3$ ,  $H_0 = 70 \text{ km s}^{-1} \text{ Mpc}^{-1}$ ) is used throughout this paper.

## 2 Classification scheme

In order to collect a sample of early-type galaxies, we started with a pre-selection of the candidates. Figure 1A shows the values of concentration (defined as in Bershady et al. 2000) and  $M_{20}$  (Lotz et al. 2004) for all source detections with  $i_{AB} \leq 24$ . The galaxies are distributed in this  $C - M_{20}$  space along a ridge which shows two slopes, with a knee at a concentration  $C \sim 2.4$ . Simulations show that this is the trend expected for a range of Sersic surface brightness profiles with the most concentrated indices ( $n \sim 3 - 4$ ) living in the upper-right region of the diagram. Early-type galaxies have higher concentrations, and the varying slope suggests a transition between the steep  $R^{1/4}$  profiles of elliptical galaxies and the exponential profiles of disks. Objects with concentration  $C > 2.4$  were pre-selected and visually inspected by four of us (IF, TL, CMC and SJL). The final sample of visually classified early-types comprise 380 objects. However, a visually classified sample

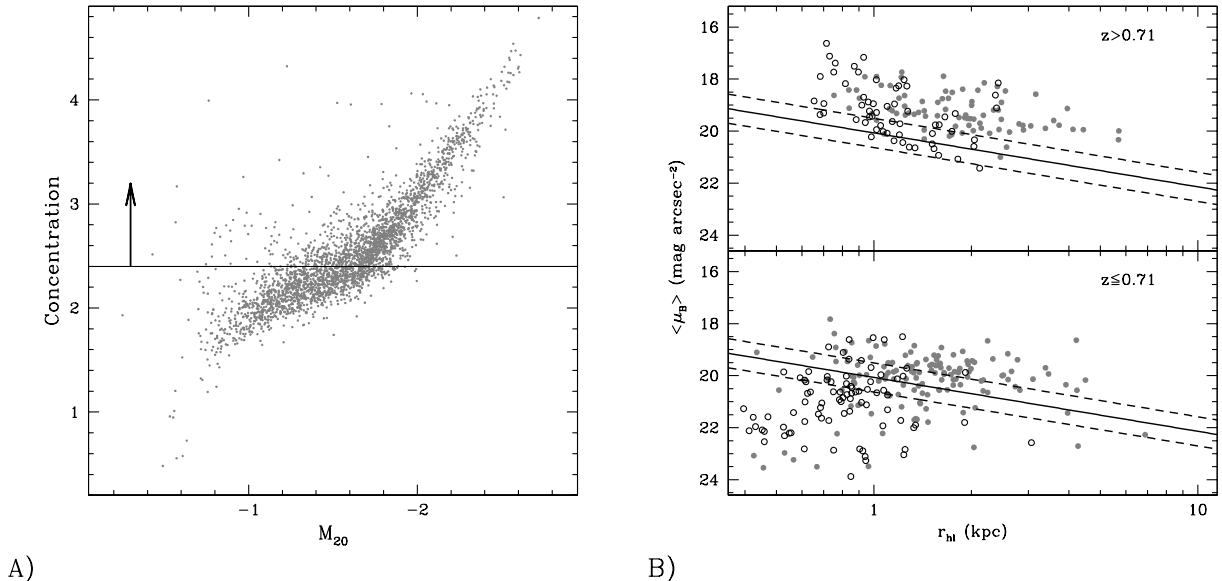


Figure 1: **Selection of early-type galaxies.** *LEFT:* Sample pre-selection based on the surface brightness distribution. Galaxies with  $C > 2.4$  were visually inspected. *RIGHT:* The Kormendy relation is shown for the galaxies visually classified as early-types. The local Kormendy relation is shown as a solid line, including the scatter (dashed lines).

will be contaminated by late-type galaxies which appear concentrated. Such is the case for bright knots of star formation within a galaxy with an overall faint surface brightness.

Our main goal is to select a sample that resemble today’s elliptical galaxies. Needless to say, such a sample is affected by the progenitor bias (van Dokkum & Franx 2001) which implies that stars in galaxies with a non early-type morphology can end up in elliptical galaxies by  $z = 0$ . Other catalogues of distant early-type galaxies suffer from other types of biases. For instance, the large sample of COMBO 17 galaxies (Bell et al. 2004) specifically target red galaxies. It is a combination of these different selection processes that allow us to obtain a complete picture of the evolution of spheroidal galaxies.

For our purposes, the Kormendy relation (KR; 1977) acts as a filter. It is one of the projections of the Fundamental Plane and does not require spectroscopy. The KR has been found to hold in early-type galaxies out to moderate redshifts (La Barbera et al. 2003). The KR of the selected candidates is shown in figure 1B<sup>1</sup>. Filled and open circles correspond to galaxies with red/blue colours, respectively<sup>2</sup>. The selected galaxies are shown with respect to their rest frame B-band surface brightness. Redshifts for the K-corrections were obtained from the photometric redshift catalogue of Mobasher et al. (2004)<sup>3</sup>. These galaxies are at redshifts  $z \lesssim 1$ , corresponding to a lookback time  $\Delta t \lesssim 8$  Gyr. In order to compare them with the local KR – shown as a solid line, including the scatter as dashed lines – we must consider that the stellar populations will fade as the galaxies evolve with time.

Hence, those sources falling below the local relation (solid line) will “drift away” from the Kormendy relation and can thus be rejected as galaxies that will not evolve *by stellar evolution* into this relation. The final sample comprises 249 galaxies over the 160 arcmin<sup>2</sup> field of view. Figure 2 shows the sample properties: The  $V - i$  colour, half-light radius and rest-frame  $V$ -band absolute luminosity are shown as a function of redshift. The lines in the left panel are predictions from the population synthesis model GALAXEV (Bruzual & Charlot 2003) assuming an exponentially decaying star formation rate at fixed (solar) metallicity, with timescales 0.5 (solid), 1 (dashed) and 8 Gyr (dotted). The filled and hollow circles represent red/blue galaxies according to integrated photometry. Most of the early-type galaxies (selected irrespective of colour) are old, passively evolving systems, with just 20% of galaxies with blue colours which could represent either a later formation epoch or a secondary episode of star formation. The bluer galaxies tend to be smaller and fainter. It is interesting to notice that most of the candidates rejected by the “Kormendy filter” described above are small objects at redshifts  $z < 0.5$ . Splitting the sample about the median redshift  $z = 0.7$ , one finds that the fraction of blue early-types decreases from 35% at  $z > 0.7$  to 10% at  $z < 0.7$ .

<sup>1</sup>The figure shows the B-band surface brightness in the rest frame, including the  $(1+z)^4$  cosmological dimming term.

<sup>2</sup>The separation between red and blue galaxies is based on the best fit from the photometric redshift catalogue. Roughly, red galaxies have colours characteristic of local E/S0/Sa galaxies. See Ferreras et al. (2005) for details.

<sup>3</sup>One third of the galaxies have spectroscopic redshifts from the ESO/VLT follow-up observations (Le Fèvre et al. 2004; Vanzella et al. 2005).

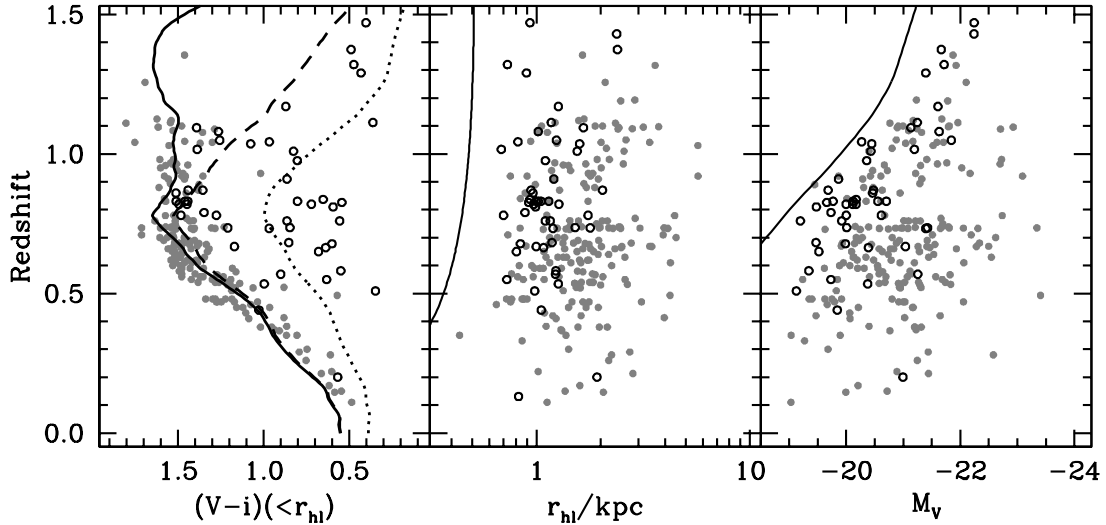


Figure 2: **GOODS-S Early-type sample.** The colour, size and absolute luminosity are shown as a function of redshift. The solid lines in the middle and right panels are limiting values from the detection process. The lines in the left panel represent an exponentially decaying star formation rate (solar metallicity), started at  $z_F = 5$  with a decay timescale of 0.5 (solid), 1 (dashed) and 8 Gyr (dotted). Bruzual & Charlot (2003) models are used.

### 3 The formation of early-type galaxies

Despite the small field of view (160 arcmin<sup>2</sup>) one can set constraints on the evolution of the number density of early-type galaxies out to  $z \sim 1$ . Figure 3A shows the comoving number density as a function of redshift, with the error bars including both Poisson noise and the effect of cosmic variance. The latter is estimated from Somerville et al. (2004) for the volumes probed by the sample, assuming a correlation function  $\xi(r) = (r_0/r)^\gamma$ , with  $r_0 = 5h^{-1}$  Mpc and  $\gamma = 1.8$ . The dots comprise all galaxies with absolute magnitude  $M_{B,*}(z) \pm 1$  mag, where  $M_{B,*}(z)$  gives the rest-frame B-band absolute luminosity of a typical galaxy at a given redshift. It is computed by constraining  $M_{B,*}(z = 0)$  to the local luminosity function and using a 0.5 Gyr exponentially decaying SFR along with the Bruzual & Charlot (2003) models to track the evolution with redshift. The shaded area illustrates the point that a zero-evolution scenario is still compatible with the data. However, if we include the  $z = 0$  point corresponding to the local density of E/S0s from Marzke et al. (1998), we find a significant evolution between  $z = 0$  and 1. Three lines sketch a simple power law behaviour of the density:  $\phi_*(z) \propto (1+z)^{-\beta}$ , with  $\beta$  in the range 2-4.

The depth and spatial resolution of the ACS images allow us to perform a resolved colour analysis of the sample. We find a remarkable correlation between the integrated colour and the colour gradient, so that red galaxies tend to have red cores and vice-versa. The large range spanned in lookback times in our samples can be used to explore the mechanism behind the colour gradients. Selecting the subsample of galaxies with red cores, we show in figure 3B the redshift evolution of the  $V - i$  colour gradient (top) and scatter (bottom). The lines follow the evolution of simple models calibrated to the local ( $B - R$ ) colour gradients from the sample of Peletier et al. (1990). The solid line assumes the colour gradients are explained by a range of metallicities, whereas the dashed lines assumes a range of ages. As expected, the age-sequence evolves very quickly: In this model, the blue, outer regions have younger stars which evolve faster than the inner parts, increasing the slope with redshift. The metallicity-model assumes that the blue, outer regions have similar ages but lower metallicities. This implies the inner and outer regions evolve "in synch", resulting in a milder evolution of the colour gradient. The data are compatible with a pure metallicity sequence. The scatter does not evolve with redshift. Figure 3A and 3B show a very interesting dichotomy. The photometric properties (3B) are typical of systems formed very early, followed by passive evolution, whereas the number density (3A) suggests a significant evolution.

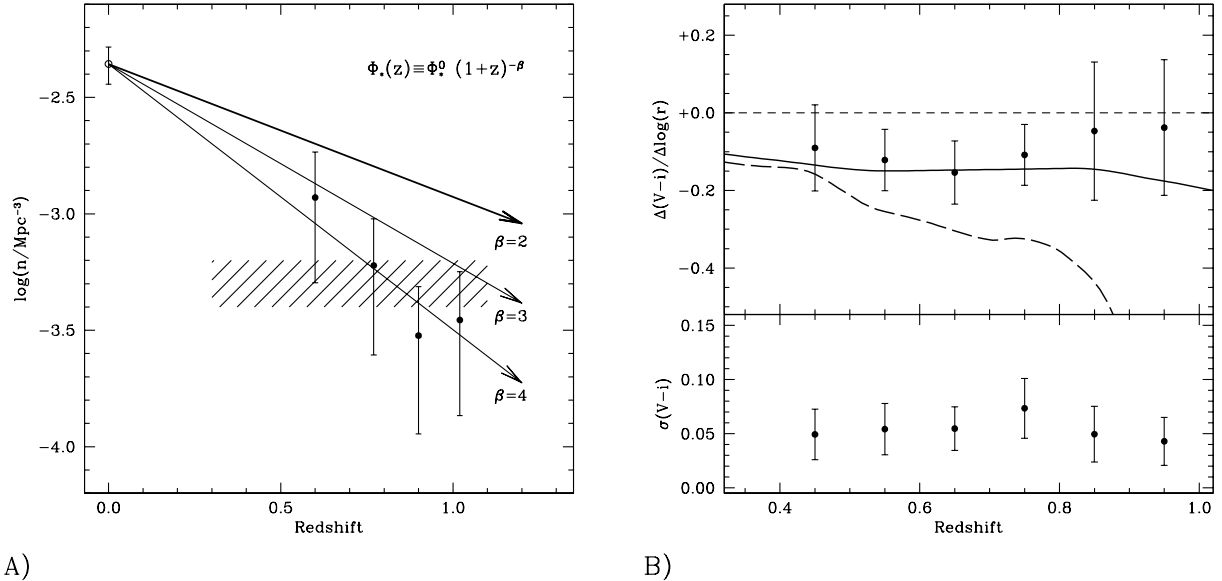


Figure 3: **The evolution of early-type galaxies.** *LEFT*: Evolution of the comoving number density compared to simple power laws. The  $z = 0$  point corresponds to the local E/S0 luminosity function (Marzke et al. 1998). The error bars take into account Poisson noise and cosmic variance. *RIGHT*: Evolution of the colour gradient and scatter. The solid (dashed) line corresponds to a model that relates the *local* colour gradient of ellipticals to a range of metallicities (ages).

## 4 UDF and the structure of distant early-type galaxies

The depth of the UDF images allowed us to explore in detail the surface brightness distribution of some of the early-type galaxies from the GOODS sample. Figure 4A shows the structural parameter  $\langle a_4/a \rangle$  which measures the deviation of the isophotes from pure elliptical shapes. Positive/negative values of  $\langle a_4/a \rangle$  imply disk/boxy isophotes, respectively. Our UDF sample is shown as black dots with respect to half-light radius, ellipticity or rest-frame B-band absolute luminosity. The grey dots correspond to the local sample of Bender et al. (1989). The figure suggests an early and uneventful morphological evolution of early-type galaxies. Similarly to nearby elliptical galaxies, our moderate redshift sample also correlates diskyness/boxyness with faint/bright luminosities, respectively.

However, a detailed analysis of the isophotes reveals some interesting features: figure 4B shows two of the 18 spheroidal galaxies observed. Their  $V-i$  colour maps are shown in the left panels. Both objects are typical “red and dead” galaxies with red cores. The central panels give the best fit for a homogeneous surface brightness distribution ( $i$  band), using the IRAF task ELLIPSE (Jedrzejewski 1987). The right panels are the residuals with respect to these fits. While J033244.09-274541.5 (top) shows no significant residual, UDF 2387 presents a remarkable signature suggesting a recent dynamical event, possibly a merger.

## 5 Assembling the puzzle

We have assembled a sample of intermediate-redshift galaxies which – by construction – already look like today’s elliptical galaxies. Such approach has the advantage of not relying on colour selection which will bias the sample in favour of the old stellar populations seen in local early-type systems. Given the depth and spatial resolution of the ACS images, this sample robustly comprises all galaxies which can be expected to evolve into local early-type systems. One could still argue that the “filter” applied regarding the Kormendy relation will bias against other possible progenitors. Unfortunately, such an analysis cannot rely on a morphological estimation. Furthermore, the small scatter of the colour magnitude relation at  $z = 0$  (e.g. Terlevich, Caldwell & Bower 2001) implies that blue galaxies in the redshift range pertinent to this sample,  $z \lesssim 1$ , are unlikely progenitors of today’s elliptical galaxies. The evidence gathered from this sample presents morphologically-selected early-type galaxies as mostly made up of an old, passively evolving population, where the colour gradients are purely caused by a range of metallicities. The fraction of blue galaxies increases with redshift and corresponds to fainter systems (i.e. ‘downsizing’), but stays overall at a low fraction, around 20%. On the other hand, the comoving number density presents a significant decrease with redshift, suggesting either a strong evolution of the assembly history as predicted by hierarchical models, or a selection bias caused by dust.

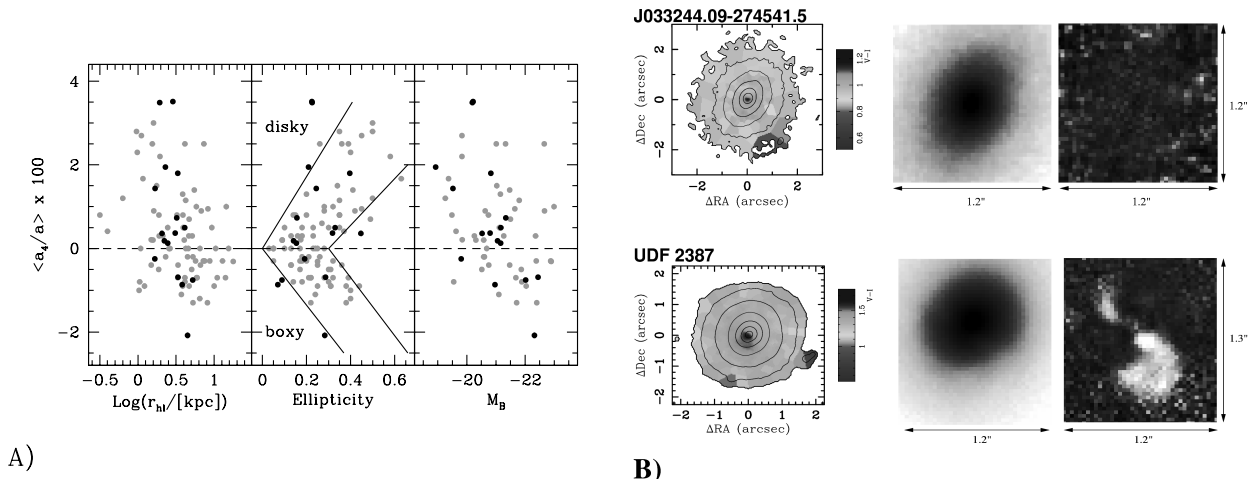


Figure 4: **Detailed structure from the UDF.** *LEFT:* The structural parameter  $\langle a_4/a \rangle$  measures the diskiness/boxyness of a galaxy. The black dots are UDF early-type galaxies, which are very similar to the local sample of Bender et al. (1989; grey dots) *RIGHT:* Two early-type galaxies from the UDF images. The left panels show the  $V - i$  colour maps; the middle panels give the best fit to a smooth surface brightness profile (in the  $i$  band). The right panels give the residuals. Both galaxies have red cores and do not show any appreciable photometric departure from a “standard” early-type galaxy.

## References

- [1] Bell, E., et al. 2004, ApJ, 608, 752
- [2] Bender, R., et al. 1989, A&A, 217, 35
- [3] Bershady, M. A., Jangren, A. & Conselice, C. J., 2000, AJ, 119, 2645
- [4] Bruzual, G. & Charlot, S., 2003, MNRAS, 344, 1000
- [5] Ferreras, I., Lisker, T., Carollo, C. M., Lilly, S. J. & Mobasher, B., 2005, ApJ, in press, astro-ph/0504127
- [6] Förster-Schreiber, N. et al. 2004, ApJ, 616, 40
- [7] Giavalisco, M. et al. 2004, ApJ, 600, L93
- [8] Jedrzejewski, R. I., 1987, MNRAS, 226, 747
- [9] Kormendy, J., 1977, ApJ, 218, 333
- [10] La Barbera, F., et al. 2003, ApJ, 595, 127
- [11] Le Fèvre, O, et al., 2004, A&A, 428, 1043
- [12] Lotz, J. M., Primack, J. & Madau, P., 2004, AJ 128, 163
- [13] Marzke, R. O., et al. 1998, ApJ, 503, 617
- [14] Mobasher, B, et al. 2004, ApJ, 600, L167
- [15] Pasquali, A., Ferreras, I., et al. 2005, ApJ, in press, astro-ph/0504264
- [16] Peletier, R. F, et al., 1990, AJ, 100, 1091
- [17] Somerville, R. S., 2004, ApJ, ApJ, 600, L171
- [18] Terlevich, A. I., Caldwell, N. & Bower, R. G., 2001, MNRAS, 326, 1547
- [19] Thomas, D. 1999, MNRAS, 306, 655
- [20] Treu, T. et al. 2005, ApJ, 622, L5
- [21] van Dokkum, P. G. & Franx, M., 2001, ApJ, 553, 90
- [22] Vanzella, E., et al. 2005, A&A, 434, 53
- [23] White, S. D. M. & Rees, M. J. 1978, MNRAS, 183, 341